International Immunology, Vol. 16, No. 8, pp. 1133–1142
doi:10.1093/intimm/dxh113 Advance Access publication 5 July 2004

A novel reticular stromal structure in lymph node cortex: an immuno-platform for interactions among dendritic cells, T cells and B cells

Tomoya Katakai[1], Takahiro Hara[1], Jong-Hwan Lee[1], Hiroyuki Gonda[1,2], Manabu Sugai[1] and **Akira Shimizu[1,2]**

[1]Center for Molecular Biology and Genetics, Kyoto University and [2]Translational Research Center, Kyoto University Hospital, Kyoto 606-8507, Japan

Keywords: CCL21, fibroblastic reticular cells, lymphoid tissue, PNAd, reticular network, stromal cells

Abstract

For efficient adaptive immunity, the lymph nodes (LNs) are equipped with a strategically organized microarchitecture, which is largely supported by the reticular network (RN). The RN can be clearly visualized by fluorescence immunohistochemistry coupled with confocal imaging using a monoclonal antibody, ER-TR7, and can be subdivided into four structurally distinct regions, each of which correlates well with the location of distinct immune cell subsets. In addition, we noticed a characteristic reticular structure designated the 'cortical ridge' at the boundary of the T and B zone, in which dendritic cells are preferentially accumulated. *In vitro* adhesion assays of frozen sections demonstrated a preference of dendritic cells for the cortical ridge rather than the deeper cortex. Adoptive transfer experiments also demonstrated that antigen-bearing dendritic cells migrated to this region from peripheral tissues, especially in the vicinity of the high endothelial venules, and were anchored on the reticular fibers waiting to interact with the antigen-specific T cells. Taken together, the findings obtained in this study provide new insights into how the LN stromal reticulum works as a specialized 'immuno-platform' for tissue compartmentalization and the immune response.

Introduction

Lymph nodes (LNs) are a kind of secondary lymphoid tissue located at the downstream neck of the lymphatic system, which carries lymph drained from peripheral tissues; LNs monitor and filter the tissue fluid exudate as part of the mechanism of achieving an efficient adaptive immune response (1–3). Within a LN, distinct subsets of immuno-hematopoietic cells are strategically compartmentalized to form a unique micro-architecture (2–4). Strikingly, B and T lymphocytes are clearly separated at the cortical region. B cells are organized into primary follicles within the outer cortex (B zone), and occasionally develop germinal centers (GCs) during T cell-dependent immune responses. A majority of T cells reside in the paracortex (T zone). Dendritic cells (DCs) carrying information from the peripheral tissues and arriving at the subcapsular sinus (SCS) through afferent lymphatics further migrate into the T zone to interact with T cells (5). Several macrophage subsets are distributed mainly at the medulla and SCS regions, where lymphocytes are relatively sparse (6).

The localization of immune cells within the LN is regulated by various chemokines and adhesion molecules expressed on stromal populations (4). In particular, homeostatic chemokines such as CCL19, CCL21, CXCL12 and CXCL13 have several especially important roles (4). Stromal cells, including endothelial cells, follicular dendritic cells (FDCs) and fibroblastic reticular cells (FRCs), provide a functional scaffold for the migration of immune cells by forming a chemoattraction and adhesion milieu. FRCs are the cells responsible for building a complicated reticular network (RN) by producing various extracellular matrix components and interweaving them to make reticular fibers (RFs) (6–10). The RN covers a large part of the LN and is considered to support the tissue mechanically as well as to provide spaces for the locomotion of immune cells. However, the actual functional roles of the FRC/RN in immune responses have long been elusive. Recent studies by Shaw and colleagues have thrown light on a subset of RN functions and led to the proposal of an intriguing

Correspondence to: T. Katakai; E-mail: tkatakai@virus.kyoto-u.ac.jp

Transmitting editor: T. Kurosaki

Received 22 December 2003, *accepted* 18 May 2004

concept in which reticular microstructures such as the 'paracortical cord (PCC)' and 'conduit' are considered to be an integrated system (7,8). The PCC is a structural unit of the postcapillary vessel/high endothelial venule (HEV) with associated concentric RN in the T zone, while the reticular conduit is an electron microscopic-scale narrow path of RF space ensheathed by FRC. They also showed that the PCC actually functions as the transporting machinery by which low molecular weight materials are brought from the SCS up to the HEV through the conduit, and thus it may have an impact on lymphocyte homing (9). However, there still remain many unclear issues regarding the LN reticular stroma. Precisely identifying the microanatomical sites (including the underlying stromal milieu) in the LN where the immune response is in progress will help to advance our understanding of various infections, allograft rejection, autoimmune diseases and tumor metastasis. Accordingly, characterization of the cellular and molecular nature of the RN and its roles in the immune response are important issues at present.

In this study, we obtained clear microscopic images of the LN reticular stroma. Analysis of these images revealed that the features of the RN vary in accordance with the LN subcompartments for immune cell subsets. In addition, we found a novel stromal structure, the cortical ridge, at the boundary of the T and B zones, where DCs preferentially migrate and accordingly, T–DC interactions frequently take place. These observations suggest that the RN and immune cell subsets cooperatively construct a specialized stromal milieu, and in particular the cortical ridge is a specialized reticular stromal structure supporting DC–T–B interactions.

Methods

Mice and immunization

BALB/c mice (purchased from Japan SLC Inc., Shizuoka, Japan) and a transgenic mouse line carrying an ovalbumin ($OVA_{323–339}$)-specific TCR gene on a BALB/c background (11) were maintained at the Center for Molecular Biology and Genetics, Kyoto University. Mice were immunized subcutaneously with 100–200 μg of OVA in a 1:1 mixture of PBS and alum adjuvant (Inject Alum, Pierce, Rockford, IL) or in a 1:1 emulsion of PBS and complete Freund's adjuvant (CFA) (Difco, Detroit, MI) in the footpads.

Antibodies

The antibodies used were as follows: as primary reagents, anti-ER-TR7 (BMA, Augst, Switzerland), biotin–anti-CD3, biotin–anti-CD4, FITC–anti-B220, anti-CR1, FITC–anti-CD11c, PE–anti-CD44, FITC–anti-CD45RB, biotin–anti-CD80, anti-DX5, anti-PNAd (PharMingen, San Diego, CA), anti-PECAM-1, anti-L-selectin (Caltag, Burlingame, CA), anti-Mac-1 (Immunotech, France), anti-CCL21 (R&D, Minneapolis, MN), anti-gp38 (clone 8.1.1, ref.12), anti-FcγRII/III, anti-MHC classII and anti-CD8 antibody (hybridoma supernatants); as secondary reagents, FITC-, PE-, APC-, or biotin–anti-rat IgG, FITC-, PE-, or APC–streptavidin, FITC–anti-hamster IgG (Caltag) and biotin–anti-rat IgM (PharMingen).

Immunohistochemistry and fluorescence microscopy

LNs were isolated from mice, embedded in OTC compound (Sakura Finetechnical, Tokyo, Japan), and then frozen in liquid nitrogen (13). After the frozen sections (10 or 60 μm) were fixed with cold acetone or 3% paraformaldehyde–PBS for 5 min, they were treated with PBS supplemented with 1% BSA and 5% mouse serum for blocking. Sections stained with antibodies by direct or indirect methods were examined using a confocal laser scanning microscope (MRC-1024, Bio-Rad Labs, Osaka, Japan) or a fluorescence microscope (TND330, Nikon, Tokyo, Japan) with a 3CCD camera (C5810, Hamamatsu Photonics, Hamamatsu, Japan). Digital images obtained were prepared using Adobe Photoshop software (Adobe Systems Inc., San Jose, CA).

Cells

$CD4^+$ cells were prepared from peripheral LNs from BALB/c or transgenic mice as the bound fraction obtained using a magnetic cell sorter (Miltenyi Biotec, Bergisch Gladbach, Germany) with biotin–anti-CD4 antibody (PharMingen) followed by streptavidin–MicroBeads (Miltenyi Biotec). For the separation of naive and memory $CD4^+$ T cells, negative selection by the magnetic sorting using antibodies against MHC class II, FcγRII/III, B220, Mac-1, CD8 and Dx5 followed by positive selection using anti-L-selectin was performed.

DCs were generated as described previously with some modifications (14,15). In brief, bone marrow cells from BALB/c mice tibias and femurs were suspended in 10% FCS–RPMI medium and incubated in a tissue culture dish for 2 h. Non-adherent cells were replated onto a non-tissue culture dish with 10% FCS–RPMI containing recombinant murine GM-CSF (10 ng/ml, Peprotech Inc., Rocky Hill, NJ) and IL-4 (10 ng/ml, Peprotech). On days 3 and 6, the medium was replaced by fresh, factor-containing medium. On day 8 or 9, the cells were used for experiments as DCs. For DC stimulation, LPS (20 μg/ml) with or without OVA (50 μg/ml) was added to the culture before 24 h (before the cells were harvested for experiments). The differentiation of DCs was confirmed by flow cytometric analysis for CD11c, MHC classII and CD80 expression using a FACScalibur flow cytometer with Cell Quest software (Becton Dickinson).

Frozen section adhesion assay

DCs' adhesion to LN sections was assessed by an *in vitro* frozen section assay as described previously (16,17) with some modifications. DCs labeled with CDFDA were suspended at $1–2 \times 10^5$ cells/150 μl in complete medium and overlaid onto 16-μm-thick, unfixed frozen sections of peripheral LNs mounted on glass slides. The assay was performed at 37°C for 30 min in a static condition. After removal of nonadherent cells by gentle washing with complete medium, sections were fixed in 3% paraformaldehyde–PBS and then stained for ER-TR7.

Adoptive transfer

2×10^5 OVA-pulsed mature DCs labeled with CDFDA (Molecular Probes, 37°C, 20 min) and 1×10^7 OVA-specific $CD4^+$ T cells labeled with CMTMR (Molecular Probes) were

injected subcutaneously and intravenously, respectively. LNs were isolated at various time points for immunohistochemistry.

CR-preference index

Images of the LN outer cortical region that contained capsule, follicles, CRs and T zones were obtained in many different parts of the LN sections. Outer (SCS and B zone side) and inner (T zone side) boundaries of the CR were traced according to the structural characteristics revealed by ER-TR7 staining, and the total pixel sizes (in pixels) of each area were computed using NIH Image version 1.62 software (National Institutes of Health). Then, fluorescence-labeled cells in each area were counted. Since areas of subregions and total cell numbers in different images varied considerably, it was necessary to calculate cell density per unit area or the ratios of values to compare two regions within an image or different images, respectively. For this reason, 'CR-preference index' was calculated using the following formula: [cell number in CR / CR size (pixels)] / [cell number in deeper cortex / deeper cortex size (pixels)]. This numerical value represents the ratio of cell density in the CR to that in the deeper T zone on an image. Therefore, an index number over '1' indicates that there is some preference for the CR compared to the deeper T zone.

Results

RN subcompartments in the LN

To visualize the LN reticular structure with high resolution, we performed fluorescence immunohistochemistry coupled with confocal imaging. A monoclonal antibody, ER-TR7, which recognizes an undetermined fibroblast antigen (18), clearly visualized the RN in the LN (Fig. 1). Although the RN extended throughout the LN, local aspects of the architecture were uneven, and hence we were able to subdivide it into four major subcompartments (Fig. 1B). (i) Subcapsule-associated RN (SC-RN): SCS-supporting structures including the capsule and several layers of reticulum placed just below the SCS-lining floor. Especially, the interfollicular channel (IFC) region, a special site located between two follicles from which the strands of RFs penetrate into the T zone, is noteworthy for later discussion. (ii) B cell-associated RN (B-RN): relatively sparse RFs that are mainly associated with follicular capillary vessels, and thereby form an apparently rough network inside the follicle. This area is occupied chiefly by the FDC network (not shown) rather than RFs. (iii) T cell-associated RN (T-RN): orderly arranged lattice-like network widely distributed in the paracortex and precisely overlapping to the T cells' location. Basically, blood vessels are enwrapped by the FRC bundles, and are thus detected as tube- or ring-forming ER-TR7-stained structures on the sections. Among these structures, those with larger diameter correspond to the HEV-associated bundles. Most HEVs are also clearly encircled by concentric or spiral RF strands, demonstrating that the PCC system is well visualized by ER-TR7 staining. (iv) Medullary RN (M-RN): extensively branched MCs, inter-connected blood vessels with associated column-like structure of RN, construct a complicated cord-and-sinus system in the medulla, which is hence an RN-concentrated environment. These images vividly reveal the RN subcompartments and provide further structural details that are well consistent with the already outlined LN microanatomy (2,4).

Cortical ridge is a notable stromal structure at T/B boundary

Apart from the above large-scale reticular architecture, we noticed that a characteristic stromal structure was often constructed at the boundary between the T and B zones (Fig. 1). It was a relatively vessel- and RN-rich belt-like zone extending from the IFC and running along the paracortical side of the follicular edge. HEVs were frequently seen in this region. We named this remarkable structure the cortical ridge (CR), since it seemed to separate the T and B zones. In the LN sections, one IFC with two CRs beneath the respective two follicles gave rise to a typical fan-shaped area around the junction of three cortical RN structures, SC-RN, B-RN and T-RN. We often observed that the PCC across the T zone finally connected to the CR, suggesting that the CR is a tip of the PCCs in which they fuse or split (Fig. 1B and C). It is also worth noting that the CR appears to be directly connectable to the medulla, since we often observed that it extended from the medulla beneath the follicles located near the cortico-medullary (C-M) junction (Fig. 1B and C, asterisks).

HEVs are known to express a homeostatic chemokine, CCL21, and a carbohydrate antigen, PNAd, which are the two best-studied functional landmarks for the HEVs and play crucial roles in lymphocyte homing to LNs via counter receptors CCR7 and L-selectin, respectively (19,20). DCs also acquire responsiveness to CCL21 in the course of maturation, which is the major cause of their movement to the T zone (4,21). We found that the two molecular markers expressed by the HEV endothelial cells were also concentrated on the RNs that associate with the CR as well as the PCC (Fig. 2). This suggests that the RNs in such specialized areas slightly differ from other RNs with regard to characteristics associated with the control of immune cells' migration. It is likely that the CR stroma acts as a strong attractor for DCs or T cells expressing CCR7.

DCs are preferentially accumulated in the CR

In order to observe the location of LN-resident DCs, LN sections from unsensitized animals were stained for CD11c together with ER-TR7 and CD3. Strikingly, $CD11c^+$ DCs were apparently accumulated in the CR, compared to the deeper T zone (Figs 2A and 3A and B). These staining patterns allow us to postulate that these DCs had passed the SCS-floor at the IFC region and further migrated along with the CR-associated RFs.

To further confirm the CR preference of DCs, we performed an *in vitro* adhesion assay on frozen sections (Fig. 3C and D). When *in vitro*-differentiated DCs from bone marrow precursors were fluorescence-labeled and overlaid onto LN sections, a substantial number of cells were able to adhere to the tissue rather than the surface of the glass slide. The distribution of the bound cells within the LN was clearly uneven, and showed remarkable patterns. Basically, frequent adhesion was detected in the medulla (not shown), while the follicular B zone bound fewer DCs. SCS also appeared to bind DCs well. Importantly, we observed that DCs preferentially bound in the CR, especially in the IFC region (Fig. 3C, arrows), compared to

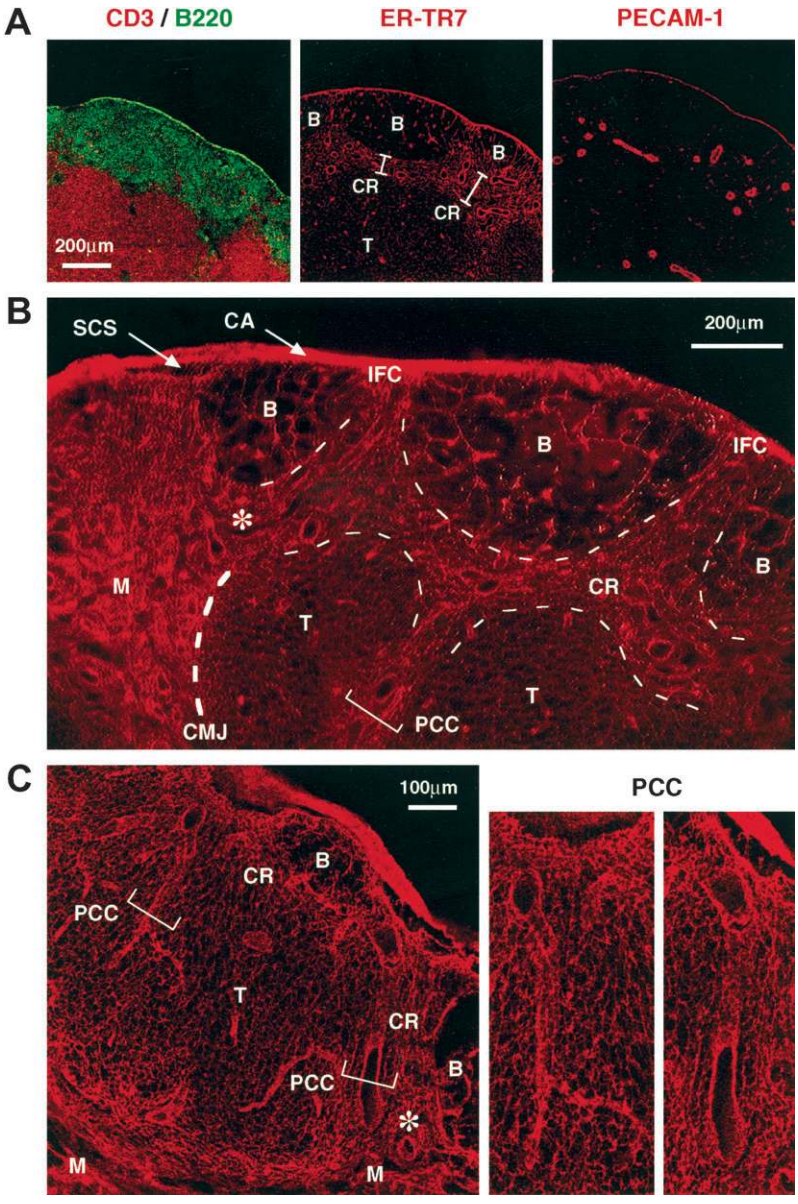

Fig. 1. RN compartments and CR in mouse LN. (A) Visualization of the correlation between the location of the lymphocyte subsets and the RN compartments, and the concentrated arrangement of blood vessels in the boundary between the T and B zones. Serial frozen sections were stained with several antibodies to detect CD3 (T cells), B220 (B cells), ER-TR7-antigen (FRCs) and PECAM-1 (endothelial cells). 'B' and 'T' in the panel with ER-TR7 staining indicate the B zone (follicle) and T zone, respectively. (B) Clear structural differences of the four major reticular subcompartments and CR revealed in a 60-μm-thick section (B, B zone; CA, capsule; CMJ, cortico-medullary junction; HEV, high endothelial venule; IFC, interfolliclular channel; M, medulla; PCC, paracortical cord; SCS, subcapsular sinus; T, T zone). (C) PCC structures run through the T zone from the deep cortex to nearby follicles. Two typical PCCs are enlarged in the right panels. Asterisks indicate channels where the CR and medulla are interconnected (B and C).

the deeper T zone. This indicates that DCs have some selective affinity for the CR. Both unstimulated (immature DC, iDC) or LPS-stimulated (mature DC, mDC) DCs showed similar binding patterns. In higher magnification views, it was evident that the bound DCs were localized on the ER-TR7$^+$-RFs.

To address whether DCs from peripheral tissues enter the LN cortex through the CR, we subcutaneously injected fluorescence-labeled DCs and collected the draining LNs. By 1 h after the injection, some DCs reached the LNs but most of them were still restricted within the SCS (Fig. 4A, arrows). In later phases, DCs were further accumulated in the SCS, especially in the IFC region, from which they penetrated into the CR reticulum (Fig. 4A, arrowheads). Collectively, these observations support the idea that the CR stroma is an initial attractor for the DCs migrating from peripheral tissues.

T cells encounter DCs in the CR with high frequency

Past studies have demonstrated that the majority of T cells enter the LN through HEVs (19,22,23). When isolated CD4$^+$

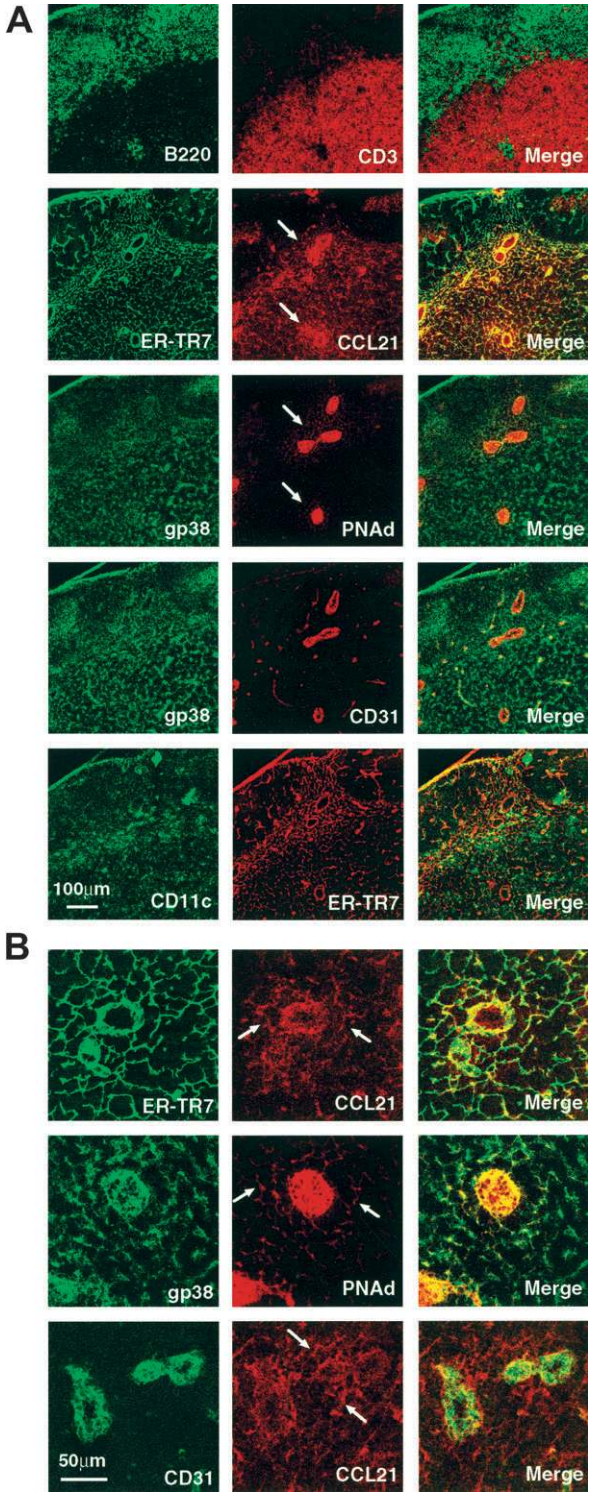

Fig. 2. CR and PCC reticula express CCL21 and PNAd. Serial frozen sections were stained for various markers. The images show a CR region (A) or PCCs (B), respectively. CCL21 and PNAd are particularly concentrated on the RN around HEVs (arrows).

T cells were transferred to recipient mice after fluorescence labeling, the T cells that rapidly homed to peripheral LNs were detectable on the sections. In accordance with our expectation, within a relatively short period after the transfer (<1 h), we were able to detect the homed T cells near the HEVs, particularly in the CR, but not yet in the deeper cortex (Fig. 4B). These images suggest the idea that the CR is a primary site for the encounter between T cells and antigen-bearing DCs after the T cells exit the HEVs. The idea was further supported by the results from a double transfer experiment in which OVA-responsive T cells and OVA/LPS-pulsed DCs were transferred into animals via intravenous and subcutaneous injection, respectively. As expected, injected DCs were preferentially localized near the CR-associated HEVs, and some of them made contact with the transferred T cells (Fig. 4C–E). Higher magnification views revealed that DCs interacting with RFs on one side were interacting with T cells on the other side (Fig. 4E). Taken together, these observations indicate that the CR reticulum is a specialized area recruiting T cells and DCs, providing a foothold for these cells and working as an efficient intermediary between them.

We next tried to determine the location of naive and memory T cells within the LN. To this end, the two types of cells isolated from mice were labeled with different fluorescent dyes for use in adoptive transfer. Consequently, we often obtained images in which memory T cells were seen to be relatively enriched in the CR as compared to the deeper cortex, while naive T cells showed no difference between the two areas (Fig. 5A and B). However, this phenomenon seemed to be rather sensitive to unknown factor(s), since there were cases in which little preference was observed. This probably means that subtle differences in the state of each LN influence the preferential localization of memory T cells in the CR. Nevertheless, this observation might imply that the CR also constitutes a specialized environment for secondary responses.

Plasticity of CR during immune responses

We finally asked whether the CR stroma changes its architecture during immune responses. To address this, mice were immunized by injecting OVA with two types of adjuvants into the footpad, and sacrificed to obtain popliteal LNs. Immunization with OVA plus alum adjuvant induced a moderate tissue swelling with large GCs concomitant with clear CR structures as compared to those in the normal popliteal LNs (Fig. 5C). It was also evident that large clusters of $CD11c^+$ DCs were formed within the CR, suggesting the enhancement of DC localization to the parafollicular sites and possibly of their survival. We frequently observed that the larger-sized follicles or follicles associated with GCs tended to be accompanied by clearer and wider CRs, thus raising the possibility that the induction of the CR might depend on B cell activation or GC development. On the other hand, immunization with complete Freund's adjuvant (CFA) induced LN enlargement far more dramatically than did alum-immunization, with gross expansion of both the T and B zones. However, the follicular structure and even the T–B boundary were disordered, and thus typical CRs disappeared. This observation again suggests that CR formation appears to depend on well-organized follicles or GCs. Interestingly, in this disorganized LN cortex, $CD11c^+$

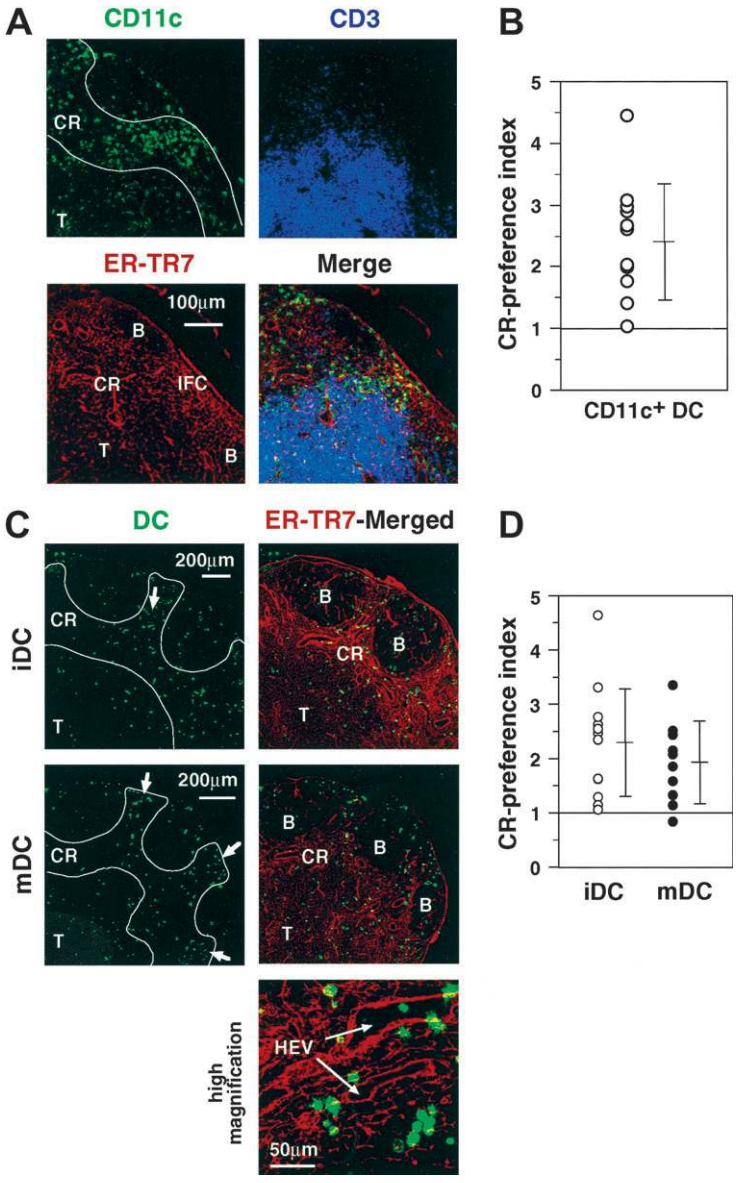

Fig. 3. DCs are accumulated in the CR. (A) $CD11c^+$ DCs are preferentially localized in the CR. Steady state LN sections were stained for ER-TR7, CD3 and CD11c. The CR region was defined by an enclosure for counting the $CD11c^+$ DCs (upper left panel). Results of calculating the CR-preferential index by $CD11c^+$ cell counting in each region are plotted in (B). The mean ±SD of multiple analyses is also shown. An index number over '1' indicates that there is some preference for the CR. (C) DCs show affinity for the CR in a frozen section adhesion assay. Fluorescence-labeled immature (iDC) or mature (mDC) DCs derived from bone marrow precursors were overlaid onto the LN sections for adhesion, and then the sections were stained with ER-TR7 after fixation. The CR-preferential indexes obtained by analyzing each image and the mean ±SD are shown in (D).

DCs were mostly accumulated on the SCS-lining floor beyond the T zone and medulla. Collectively, not only the whole RN but also the CR architecture in the LN shows great plasticity, with remodeled and possibly changed physiological character in response to lymphocyte activation during immune responses.

Discussion

In this study, we examined the detailed configuration of the LN stromal reticulum as revealed by immunostaining of ER-TR7. The RN flexibly varies its architecture according to the type of colocalized immune cell subsets (Fig. 6). This correlation is likely to be accomplished via direct interaction between the subsets and FRCs to make the specialized supporting milieu. We also characterized the CR, which is located at the boundary between the T zone and follicles and is composed of well-branched HEVs and associated RN. Various types of imaging showed that this region appears to be a crossroad for the three major agents for adaptive immunity, DCs, T cells, and B cells.

Efficient immunological communication between peripheral tissue and draining LN can be largely achieved by using DCs as a messenger (4,5). After capturing antigens, DCs leave the peripheral tissue through afferent lymphatics and finally arrive

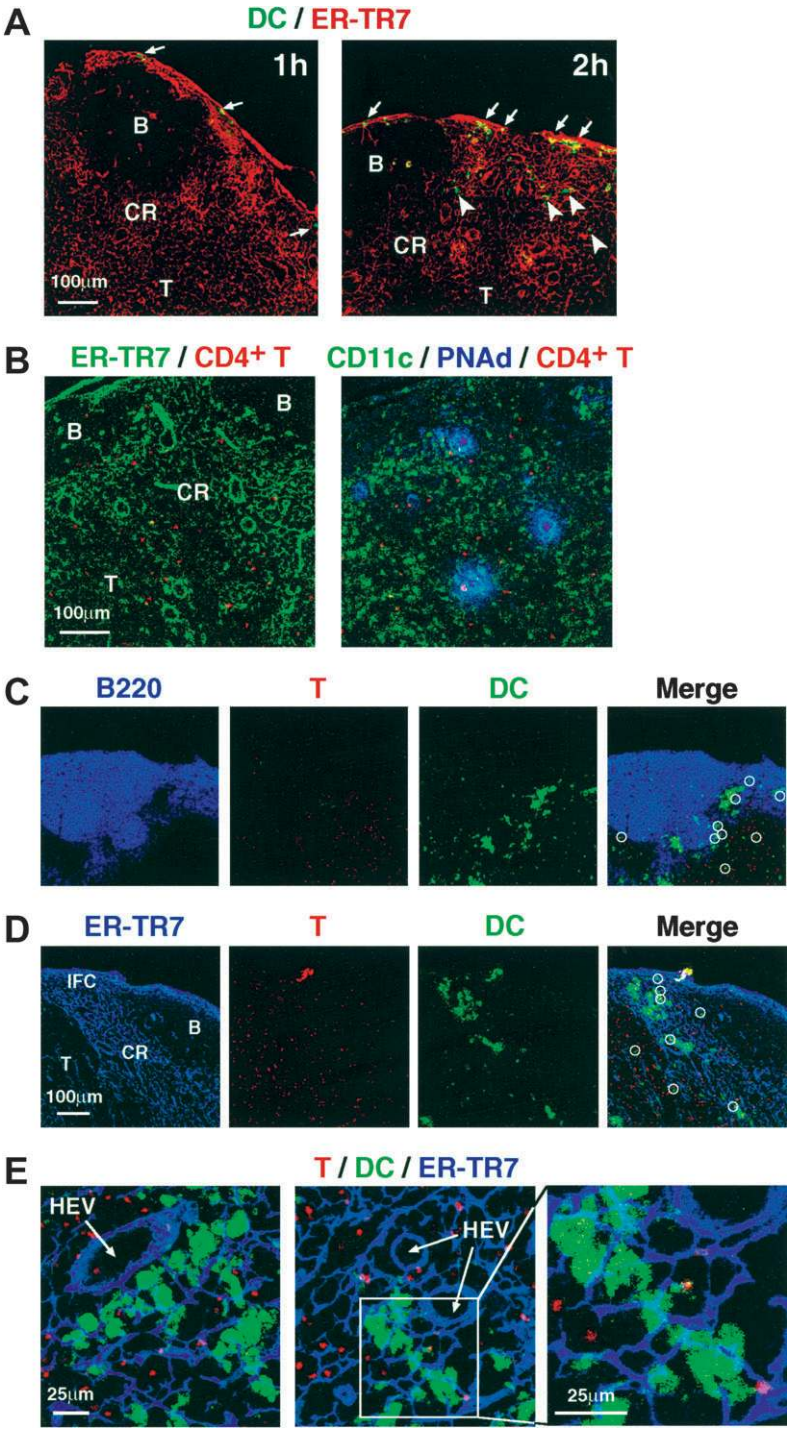

Fig. 4. T cells encounter DCs at the CR. (A) DCs from peripheral tissue enter the LN cortex through the IFC region of the CR. Fluorescence-labeled DCs were injected into the footpads of alum-immunized mice. After 1 and 2 h, draining LNs were collected and frozen sections were stained with ER-TR7. (B) T cells that exit from HEVs encounter surrounding DCs in the CR. Mice were adoptively transferred with fluorescence-labeled $CD4^+$ T cells (red), and LNs were collected 1 h after the transfer. LN sections were stained for ER-TR7, or CD11c and PNAd. (C and D) Antigen-specific T cells in contact with antigen-pulsed DCs over the RN scaffold in the CR. T–DC interactions are frequently observed in the CR (circles). OVA-specific $CD4^+$ T cells (red) and OVA-pulsed DCs (green) were transferred to mice by intravenous and subcutaneous injection, respectively, and draining LNs were collected 1 day after the transfer. The LN sections were stained for B220 (C) or ER-TR7 (D) (blue). (E) Higher magnification views, in which DCs accumulated on the RN adjacent to HEVs and waiting for T cells were observed.

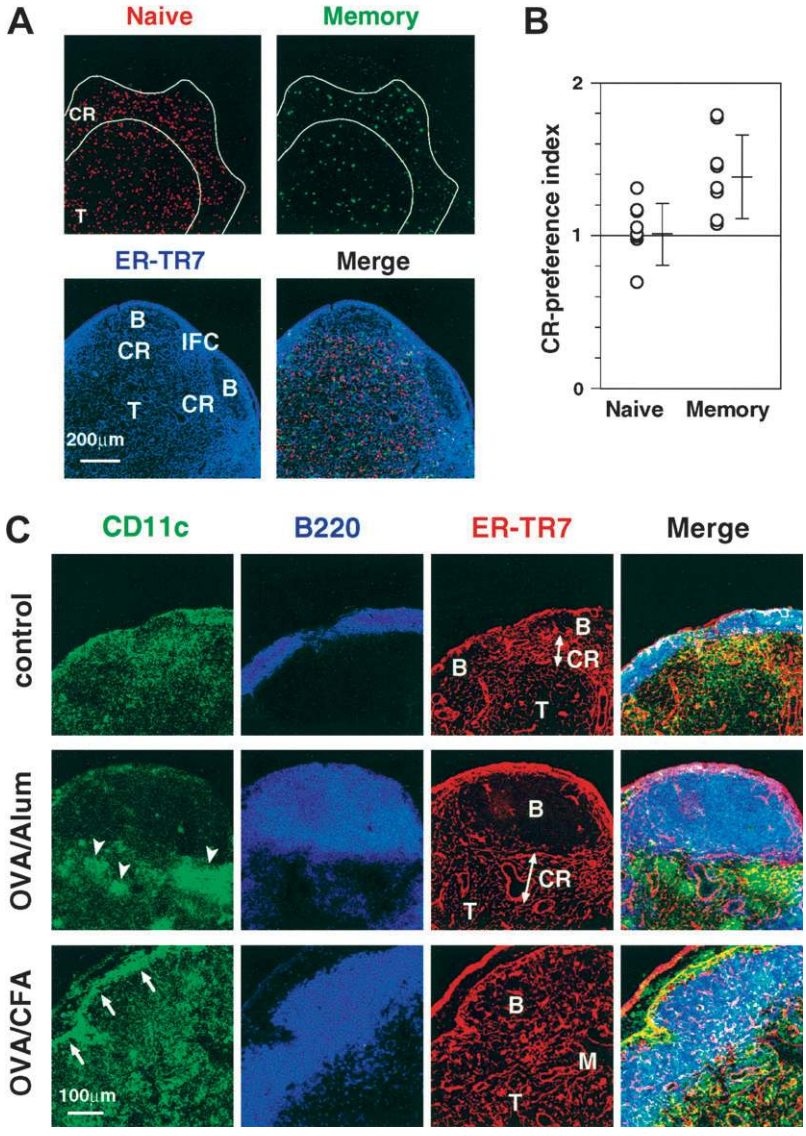

Fig. 5. (A) Memory T cells are more preferentially localized in the CR than naive T cells. Fluorescence-labeled memory (green) and naive (red) $CD4^+$ T cells were intravenously injected into mice and LNs were collected 48 h after the transfer. LN sections were stained for ER-TR7. The CR-preferential index and mean ±SD for each subset are shown in (B). (C) Dynamic remodeling of cortical RN during immune responses. Frozen sections of the popliteal LN from untreated, OVA+alum-, or OVA+CFA-immunized mice were stained with antibodies against CD11c, B220, or ER-TR7. Large clusters of $CD11c^+$ DCs were formed within the CR after alum immunization (arrowheads), while $CD11c^+$ DCs were mostly accumulated on the SCS-lining floor after CFA immunization (arrows).

at the SCS of regional LNs. These DCs are thought to further migrate across the SCS-floor lining cell layer at the IFC region and then settle at the CR to get ready for antigen presentation (Fig. 6). Its connection with the IFC suggests that the CR may act as a guideway for drawing DCs from the SCS into the T/B boundary. It is of interest that *in vitro* differentiated DCs from bone marrow precursors exhibit an affinity for the CR stroma rather than the deeper cortex, as demonstrated by assaying adhesion to frozen LN sections. This suggests that there is some specific interaction between DCs and FRCs in the CR. The CR appears to be a part of the PCC system, and for lymphocytes, it should be the major entrance point into the LN across the HEVs. After exiting the HEVs, T cells likely encounter the CR-settled DCs next in their search for specific antigens. If the antigen specificity matches, T cells would start to proliferate and maturate, whereas mismatched ones would pass through the CR and migrate further toward the medulla and finally exit the LN through efferent lymphatics. Recently, Bajénoff *et al.* reported similar results for the preferential migration of DCs near HEVs in there outer paracortex and initial T cell activation thereabout (24). Although our findings presented in this study totally accord with their observations, we provide here further information about the underlying stromal microanatomy and its potential contributions to

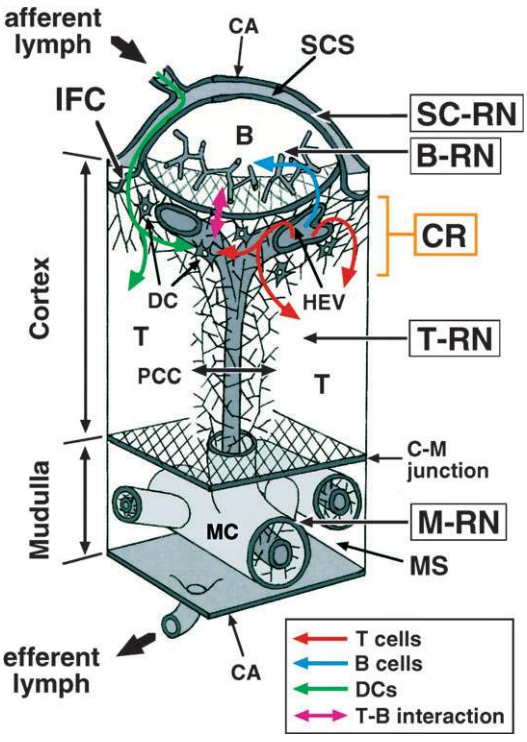

Fig. 6. Schematic representation of the LN stromal reticulum and immune effectors' trafficking. LN reticular architecture is depicted with emphasis. Four major RN subcompartments and the CR are indicated with other tissue structures. T cell-, B cell- and DC-movements as well as T–B interaction within the LN are indicated by colored arrows.

immune interactions. The conduits extending from the IFC would ensure that not only DCs but also lympho-borne low molecular weight materials are brought preferentially to the CR and associated HEVs. Chemokines are potential messengers with the role of informing circulating cells and possibly cells in the CR about the current states of peripheral tissues as well as LNs (9,25). Likewise, various cytokines produced by the peripheral tissues may stimulate FRC activity in the CR to remodel the RN or produce additional chemokines or cytokines.

LN homing events for T cells and DCs have shown to be largely dependent on CCL21 (26). Several defects in *plt* mice, in which the accumulation of naive T cells and DCs into the T zone of LNs is severely depressed, are caused by the lack of expression of lymphoid CCL21, and to some extent, the diminished expression of CCL19 (26,27). DC mobilization is prevented at the late phase of LN settling in the *plt* mice (26), suggesting that CCL21 controls the IFC-passage or subsequent migration steps toward the CR and deeper T zone. Interestingly, there is still a substantial number of DCs only around the internodular cortex (presumably the CR or IFC) of the LN in these mice (26), implying that the CR stroma produces some additional attractant for DCs. Our findings from the frozen section-binding assay strengthen this idea. Located on the boundary between three different cortical subregions, i.e. the SC-, B- and T-RN, FRCs in the CR may be stimulated by a mixture of cytokines derived from the surrounding environment. Thus, one can speculate that the CR-associated FRCs may provide a unique milieu by producing a specialized set of chemokines and adhesion molecules, which would be the attractive destination for immune effector cells in the cortex.

Additionally, we clearly showed that PCC-associated RN displayed PNAd, which has previously been shown to play a crucial role in lymphocyte attachment to the surface of HEV endothelial cells (20,28), although this phenomenon has also been reported by Bajénoff *et al.* (24). Whether PNAd is actually expressed on the PCC-associated FRC or is derived from HEVs bound to nearby FRCs has not yet been determined. However, PNAd would be a useful marker for the PCC structure.

Its position in the vicinity of the follicles is presumed to give the CR another important role. Roughly, the magnitude of each CR seemed to be correlated with the size of the adjacent B zone or GC. This observation raises the possibility that the activation of B cells might induce angiogenesis, resulting in recruitment of *de novo* HEVs with associated PCC reticulum near the follicles. Moreover, preferential antigen presentation followed by the activation of T cells inside the CR probably takes advantage of the following kinds of help for B cell activation. During T cell-dependent responses, antigen-specific B and T cell interactions occur in the paracortical side of the follicles adjacent to the T cell area (29). Recently, Relf *et al.* showed that CCL21 expressed in the T zone is involved in the movement of antigen-bound B cells toward the boundary of the T and B zone, where these cells interact with T-helper cells in the periarterial lymphoid sheath (PALS) of the spleen (30). Although there are several structural differences between the PALS and the LN, e.g. HEVs and the typical enrichment of the RN at the T/B-boundary in LNs are absent in the PALS, equivalent events probably take place in the CR of the LN. It is notable that $CD11c^+$ DCs also show the characteristic localization pattern of accumulation at the interfollicular region in splenic PALS (31). Like that in the CR, this positioning appears to be reasonable, since T cells enter the PALS through the same region and encounter the $CD11c^+$ DCs bringing blood-borne antigens, and subsequently provide efficient B cell help. In future studies, it will be interesting to examine whether the CR region retains the particular stromal structure in mice deficient for the factors important for GC development and/or lymphoid tissue structure, e.g. CD40, CD40L, TNF-α, TNFR, etc.

Taking all these findings into consideration, we conclude that the CR is the primary site for initiating efficient adaptive immune responses and that the CR reticular stroma functions as the most potent 'immuno-platform' of the LN.

Acknowledgements

We thank Dr A. G. Farr for 8.1.1 antibody; Dr T. Honjo for allowing us to use a confocal microscope; and Ms T. Ohfuji for technical assistance. This work was supported in part by Grants-In-Aid for Scientific Research on Priority Areas from the Ministry of Education, Culture, Sports, Science, and Technology of Japan.

Abbreviations

CR	cortical ridge
DC	dendritic cell

FDC	follicular dendritic cell
FRC	fibroblastic reticular cell
GC	germinal center
HEV	high endothelial venule
IFC	interfollicular channel
LN	lymph node
PCC	paracortical cord
PNAd	peripheral node addressin
RF	reticular fiber
RN	reticular network
SCS	subcapsular sinus

References

1 Zinkernagel, R. M., Ehl, S., Aichele, P., Oehen, S., Kündig, T. and Hengartner, H. 1997. Antigen localization regulates immune responses in a dose- and time-dependent fashion: a geographical view of immune reactivity. *Immunol. Revs* 156:199.

2 Young, B. and Heath, J. H. *Functional histology, fourth edition.* (Livingstone, C., London, 2000).

3 Fu, Y.-X. and Chaplin, D. D. 1999. Development and maturation of secondary lymphoid tissues. *Annu. Rev. Immunol.* 17:399.

4 Cyster, J. G. 1999. Chemokine and cell migration in secondary lymphoid organs. *Science* 286:2098.

5 Bahnchereau, J. and Steinman, R. M. 1998. Dendritic cells and the control of immunity. *Nature* 392:245.

6 Mcknight, A. J. and Gordon, S. 1998. Membrane molecules as differentiation antigen of murine macrophages. *Adv. Immunol.* 68:271.

7 Gretz. J. E., Kaldjian, E. P., Anderson, A. O. and Shaw, S. 1996. Sophisticated strategies for information encounter in the lymph node. *J. Immunol.* 157:495.

8 Gretz, J. E., Anderson, A. O. and Shaw, S. 1997. Cords, channels, corridors and conduits: critical architectural elements facilitating cell interactions in the lymph node cortex. *Immunol. Revs.* 156:11.

9 Gretz, J. E., Norbury, C. C., Anderson, A. O., Proudfoot, A. E. I. and Shaw, S. 2000. Lymph-borne chemokines and other low molecular weight molecules reach high endothelial venules via specialized conduits while a functional barrier limits access to the lymphocyte microenvironments in lymph node cortex. *J. Exp. Med.* 192:1425.

10 Kaldjian, E. P., Gretz, J. E., Anderson, A. O., Shi, Y. and Shaw, S. 2001. Spatial and molecular organization of lymph node T cell cortex: a labyrinthine cavity bounded by an epithelium-like monolayer of fibroblastic reticular cells anchored to basement membrane-like extracellular matrix. *Int. Immunol.* 13:1243.

11 Sato, T., Sasahara, T., Nakamura, Y., Osaki, T., Hasegawa, T., Tadakuma, T., Arata, Y., Kumagai, Y., Katsuki, M. and Habu, S. 1994. Naive T cells can mediate delayed-type hypersensitivity response in T cell receptor transgenic mice. *Eur. J. Immunol.* 24:1512.

12 Farr, A.G., Berry, M.L., Kim, A., Nelson, A.J., Welch, M.P. and Aruffo, A. 1992. Characterization and cloning of novel glycoprotein expressed by stromal cells in T-dependent areas of peripheral lymphoid tissues. *J. Exp. Med.* 176:1477.

13 Katakai, T., Hara, T., Sugai, T., Gonda, H. and Shimizu, A. 2003. Th1-biased tertiary lymphoid tissue supported by CXC chemokine ligand 13-producing stromal network in chronic lesions of autoimmune gastritis. *J. Immunol.* 171:4359.

14 Inaba, K., Inaba, M., Naito, M. and Steinman, R. M. 1993. Dendritic cell progenitors phagocytose particulates, including bacillus calmette–guerin organisms, and sensitize mice to mycobacterial antigens *in vivo*. *J. Exp. Med.* 178:479.

15 Labeur, M. S., Roters, B., Pers, B., Mehling, A., Luger, T. A., Schwarz, T. and Grabbe, S. 1999. Generation of tumor immunity by bone marrow-derived dendritic cells correlates with dendritic cell maturation stage. *J. Immunol.* 162:168.

16 Stamper, H. B. Jr and Woodruff, J. J. 1976. Lymphocyte homing into lymph nodes: *In vitro* demonstration of the selective affinity of recirculating lymphocytes for high-endothelial venules. *J. Exp. Med.* 144:828.

17 Wang, W.-C., Goldman, L. M., Schleider, D. M., Appenheimer, M. M., Subjeck, J. R., Repasky, E. A. and Evans, S. S. 1998. Fever-range hyperthermia enhances L-selectin-dependent adhesion of lymphocytes to vascular endothelium. *J. Immunol.* 160:961.

18 van Vliet, E., Melis, M., Foidart, J.M. and van Ewijk, E. 1986. Reticular fibroblasts in peripheral lymphoid organs identified by a monoclonal antibody. *J. Histochem. Cytochem.* 34:883.

19 Gunn, M. D., Tang, H. L., Hyman, P. L., Farr, A. G. and Cyster, J. G. 1998. A chemokine expressed in lymphoid high endothelial venules promotes the adhesion and chemotaxis of naive T lymphocytes. *Proc. Natl Acad. Sci. USA* 95:258.

20 Stein, J.V., Rot, A., Luo, Y., Narasimhaswamy, M., Nakano, H., Gunn, M. D., Matsuzawa, A., Quackenbush, E. J., Dorf, M. E. and von Andrian, U. H. 2000. The CC chemokine thymus-derived chemotactic agent 4 (TCA-4, secondary lymphoid tissue chemokine, 6Ckine, exodus-2) triggers lymphocyte function-associated antigen 1-mediated arrest of rolling T lymphocytes in peripheral lymph node high endothelial venules. *J. Exp. Med.* 191:61.

21 Dieu-Nosjean, M.-C., Vicari, A., Lebecque, S. and Caux, C. 1999. Regulation of dendritic cell trafficking: a process that involves the participation of selective chemokines. *J. Leuk. Biol.* 66,252.

22 Girard, J.-P. and Springer, T. A. 1995. High endothelial venules (HEVs): specialized endothelium for lymphocyte migration. *Immunol. Today* 16:449.

23 Kraal, G. and Mebius, R. E. 1997. High endothelial venules: Lymphocyte traffic control and controlled traffic. *Adv. Immunol.* 65:347.

24 Bajénoff, M., Granjeaud, S. and Guerder, S. 2003. The strategy of T cell antigen-presenting cell encounter in antigen-draining lymph nodes revealed by imaging of initial T cell activation. *J. Exp. Med.* 198:715.

25 Palframan, R. T., Jung, S., Cheng, G., Weninger, W., Luo, Y., Dorf, M., Littman, D. R., Rollins, B. J., Zweerink, H., Rot, A. and von Andrian, U. H. 2001. Inflammatory chemokine transport and presentation in HEV: a remote control mechanism for monocyte recruitment to lymph nodes in inflamed tissues. *J. Exp. Med.* 194:1361.

26 Gunn, M. D., Kyuwa, S., Tam, C., Kakiuchi, T., Matsuzawa, A., Williams, L. T. and Nakano, H. 1999. Mice lacking expression of secondary lymphoid organ chemokine have defects in lymphocyte homing and dendritic cell localization. *J. Exp. Med.* 189:451.

27 Luther, S. A., Tang, H. L., Hyman, P. L., Farr, A. G. and Cyster, J. G. 2000. Coexpression of the chemokines ELC and SLC by T zone stromal cells and deletion of the ELC gene in the *plt/plt* mouse. *Proc. Natl Acad. Sci. USA* 97:12694.

28 Yeh, J.-C., Hiraoka, N., Petryniak, B., Nakayama, J., Ellies, L. G., Rabuka, D., Hindsgaul, O., Marth, J. D., Lowe, J. B. and Fukuda, M. 2001. Novel sulfated lymphocyte homing receptors and their control by a core1 extention β1,3-*N*-acetylglucosaminyltransferase. *Cell* 105:957.

29 Garside, P., Ingulli, E., Merica, R. R., Johnson, J. G., Noelle, R. J. and Jenkins, M. K. 1998. Visualization of specific B and T lymphocyte interaction in the lymph node. *Science* 281:96.

30 Relf, K., Ekland, E. H., Ohi, L., Nakano, H., Lipp, M., Förster, R. and Cyster, J. G. 2002. Balanced responsiveness to chemoattractants from adjacent zones determines B-cell position. *Nature* 416:94.

31 Steinman, R. M., Pack, M. and Inaba, K. 1997. Dendritic cells in the T-cell area of lymphoid organs. *Immunol. Revs* 156:25.